

The Mouse Gene for Vascular Endothelial Growth Factor

GENOMIC STRUCTURE, DEFINITION OF THE TRANSCRIPTIONAL UNIT, AND CHARACTERIZATION OF TRANSCRIPTIONAL AND POST-TRANSCRIPTIONAL REGULATORY SEQUENCES*

(Received for publication, October 20, 1995)

David T. Shima^{‡§}, Masatoshi Kuroki[§], Urban Deutsch[¶], Yin-Shan Ng^{‡§},
Anthony P. Adamis^{§||}, and Patricia A. D'Amore^{‡§**}

From the [‡]Program in Biological and Biomedical Sciences and the ^{**}Department of Pathology, Harvard Medical School, Boston, Massachusetts 02115, the [§]Laboratory for Surgical Research, Children's Hospital, Boston, Massachusetts 02115, the [¶]Department of Ophthalmology, Harvard Medical School/Massachusetts Eye and Ear Infirmary, Boston, Massachusetts 02115, and the ^{||}Max-Planck Institut für physiologische und klinische Forschung, Bad Nauheim, Germany

We describe the genomic organization and functional characterization of the mouse gene encoding vascular endothelial growth factor (VEGF), a polypeptide implicated in embryonic vascular development and postnatal angiogenesis. The coding region for mouse VEGF is interrupted by seven introns and encompasses approximately 14 kilobases. Organization of exons suggests that, similar to the human VEGF gene, alternative splicing generates the 120-, 164-, and 188-amino acid isoforms, but does not predict a fourth VEGF isoform corresponding to human VEGF₂₀₆. Approximately 1.2 kilobases of 5'-flanking region have been sequenced, and primer extension analysis identified a single major transcription initiation site, notably lacking TATA or CCAT consensus sequences. The 5'-flanking region is sufficient to promote a 7-fold induction of basal transcription. The genomic region encoding the 3'-untranslated region was determined by Northern and nuclease mapping analysis. Investigation of mRNA sequences responsible for the rapid turnover of VEGF mRNA (mRNA half-life, <1 h) (Shima, D. T., Deutsch, U., and D'Amore, P. A. (1995) *FEBS Lett.* 370, 203–208) revealed that the 3'-untranslated region was sufficient to trigger the rapid turnover of a normally long-lived reporter mRNA *in vitro*. These data and reagents will allow the molecular and genetic analysis of mechanisms that control the developmental and pathological expression of VEGF.

The mediators of neovascularization comprise a diverse collection of growth stimulators and inhibitors that have been so designated because of their abilities to affect angiogenesis *in vivo* and/or endothelial cell proliferation *in vitro* (for review, see Ref. 1). Vascular endothelial growth factor (VEGF)¹ was initially identified based on its ability to stimulate vascular permeability (called VPF, for vascular permeability factor) and was subsequently demonstrated to be an endothelial cell-specific mitogen and angiogenic factor (2, 3). *In vivo*, VEGF expression has been correlated with embryonic, physiological, and pathological blood vessel growth (4–6). VEGF's role as a

mediator of angiogenesis has been confirmed in two distinct pathologies; VEGF has been demonstrated to be a necessary component of experimental tumor angiogenesis and tumor growth in rodents (7, 8), and, more recently, it has been shown to be causative in the development of ocular angiogenesis secondary to retinal ischemia (9, 10).

The spatial and temporal expression patterns of VEGF and its tyrosine kinase receptors, *flt-1* and *flk-1/KDR*, during periods of blood vessel growth have also led investigators to suggest a paracrine role for VEGF during the development of the embryonic vasculature (11, 12). The VEGF receptor *flk-1* is expressed in regions of the early mesoderm, which are presumed to give rise to angioblasts, and is currently the earliest known molecular marker for the endothelial cell lineage. During later stages of embryogenesis, *flt-1* and *flk-1* receptor mRNA are restricted to the endothelium of vascular cords and blood islands, with VEGF mRNA expressed in adjacent embryonic tissues (13). Proof of a role for VEGF in vessel development comes from recent studies in which VEGF receptors were deleted by targeted disruption. Mouse embryos, in which the *flk-1* receptor was deleted by targeted disruption, lacked blood islands and died between days 8.5 and 9.5. In these embryos, no organized blood vessels were observed and hematopoiesis was dramatically reduced (14). Mice, in which *flt-1* was mutated by targeted disruption, were able to form endothelial cells but unable to assemble them into normal vascular channels and thus died at mid-somite stages (15).

From these and other observations, VEGF emerges as a mediator of vasculogenic and angiogenic events associated with a wide range of biological events (16). Consistent with this concept, the local and systemic signals responsible for orchestrating the growth and regression of new blood vessels must ultimately regulate VEGF gene expression. Numerous effectors of VEGF gene expression have been identified, including cAMP, steroid hormones, protein kinase C agonists, polypeptide growth factors, oxygen, free radicals, glucose, cobalt, and iron. The potential mechanisms through which these agents modulate gene expression are varied, and include transcriptional regulation through AP-1, AP-2, steroid hormone receptors, p53, and NFκB, as well as post-transcriptional control of mRNA stability (17–21).²

To begin an analysis of the relevant mechanisms controlling the developmental and pathological expression of VEGF and to develop reagents for defining the role of VEGF in embryonic development using mouse molecular genetics, we have isolated and characterized the mouse VEGF gene. The structure of the

* This work was supported by Grant EY05985 (to P. A. D.), Massachusetts Lion's Eye Research Fund (to A. P. A.), and Research to Prevent Blindness (to A. P. A.). The costs of publication of this article were defrayed in part by the payment of page charges. This article must therefore be hereby marked "advertisement" in accordance with 18 U.S.C. Section 1734 solely to indicate this fact.

The nucleotide sequence(s) reported in this paper has been submitted to the GenBank™/EMBL Data Bank with accession number(s) U41383.

¹ The abbreviations used are: VEGF, vascular endothelial growth factor; kb, kilobase(s); PIPES, 1,4-piperazinediethanesulfonic acid; bp, base pair(s); UTR, untranslated region; LTR, long terminal repeat.

² M. Kuroki, E. E. Voest, L. V. Beerepoot, M. Tolentino, R. Y. Kim, K. A. Colby, K.-T. Yeo, and A. P. Adamis, submitted for publication.

gene was determined by restriction mapping, sequencing of intron-exon junctions, definition of the transcription initiation and termination sites, and analysis of the sequence representing the VEGF proximal promoter. Using these structural data, we have assayed the mouse VEGF gene for cis-regions responsible for different aspects of gene regulation and to this end describe gene segments sufficient to promote basal transcriptional activity and post-transcriptional regulation of the VEGF gene.

MATERIALS AND METHODS

Gene Isolation and Physical Mapping—A 129 strain mouse cosmid genomic library prepared from liver (Stratagene) was screened with random prime ^{32}P -labeled probes corresponding to the mouse VEGF₁₆₄ coding region (kindly provided by Dr. Kevin Claffey, Beth Israel Hospital, Boston). Approximately 5×10^5 colonies were screened on nylon filters (Hybond N, Amersham) by hybridizing the VEGF probe overnight at 65 °C in 500 mM phosphate, pH 7.2, 7% SDS, 1% bovine serum albumin, 1 mM EDTA, and 100 $\mu\text{g}/\text{ml}$ sheared, denatured salmon sperm DNA. Several positive clones were identified in this initial screen. After two rounds of rescreening and colony purification, cosmid DNA was isolated and analyzed by restriction digestion and Southern blot to identify useful DNA fragments for subcloning. Restriction-digested cosmid insert DNAs were subcloned into pBSII (Stratagene) for further analysis. Nucleotide sequencing of subclones indicated that VEGF cosmid clones encompassed the 3'-half of the VEGF gene (beginning near exon 4) and extended 30–40 kb in the 3'-direction.

To isolate additional clones encompassing the 5'-end of VEGF, a 280-bp cDNA probe template spanning exons 1–3 was generated, using the polymerase chain reaction, and used to rescreen 5×10^5 colonies. No additional VEGF clones were identified. As an alternative, the exon 1–3 probe was used to screen a 129 mouse genomic library in the lambda vector EMBL3 (kindly provided by Dr. Richard Moss, Brigham and Women's Hospital, Boston). The library was screened on charged nylon membranes (GeneScreen Plus, DuPont NEN) by hybridization at 42 °C in $5 \times \text{SSPE}$, 50% deionized formamide, $5 \times \text{Denhardt's}$, 10% dextran sulfate, 0.5% SDS, and 100 $\mu\text{g}/\text{ml}$ sheared, denatured salmon sperm DNA. Two positive clones were identified from screening 1×10^6 plaques. After two rounds of plaque purification, phage DNA was isolated and analyzed further. Restriction digestion and Southern blot analysis of genomic clones indicated that they encompassed the 5'-end of the VEGF gene; one clone, designated lambda 8, overlapped with cos15, a cosmid clone that terminates in the intron upstream of the exon 4 sequence. Sequence data, restriction maps, and Southern blot analysis of the mouse VEGF gene were compiled from 9- and 7.5-kb *EcoRI* subclones that encompass the VEGF coding region (see Fig. 1).

DNA Sequencing—Genomic fragments cloned into pBSII were sequenced with vector and gene-specific primers using the Sequenase 2.0 kit (U. S. Biochemical Corp.). Exon-specific primers (kindly provided by Dr. Greg Robinson, Hybridon Inc., Worcester, MA) were synthesized, based on alignment of the mouse VEGF cDNA sequence, with the published human VEGF exon structure (22). Nucleotide sequence analysis was performed with MacDNAsis 3.4 software (Hitachi).

Southern Blot Analysis—Genomic DNA was prepared from 129 mouse spleen using standard protocols (23). Restriction enzyme-digested DNA (10 μg) was electrophoresed in 0.7% TBE-agarose gels overnight. Following electrophoresis, DNA was depurinated in 0.25 M HCl, denatured, and transferred to charged nylon (GeneScreen Plus) in 0.4 M NaOH. Membranes were rinsed in $2 \times \text{SSPE}$, dried, and hybridized as described for phage library screening. The probe was a 700-bp *SmaI*-*BglI* genomic DNA fragment spanning sequences in intron 3 through intron 5 (see Fig. 1, probe A). After high stringency washes, hybrids were visualized by autoradiography.

Transcript Mapping—Total RNA isolation was performed using a modification of the acid guanidinium-phenol-chloroform extraction protocol (24) with RNazol B (Tel-test). Total RNA was further divided into poly(A)⁺ and poly(A)[−] pools, using oligo(dT) affinity chromatography (25). For primer extension, an antisense oligonucleotide primer (5'-CTGGTGAGTCCGCTGATAGTCTGCCTTGTC-3') was designed to hybridize to sequences approximately 100 bp downstream from the predicted initiation site. Primer selection and estimates of the location of the transcription initiation site were obtained by aligning mouse VEGF nucleotide sequence with the published sequence for the human VEGF 5'-untranslated region (UTR) and proximal promoter region (22). ^{32}P -End-labeled probes were separately hybridized to poly(A)⁺ and poly(A)[−] RNA obtained from normoxic or hypoxic cultures of C127I mouse mam-

mmary epithelial cells (ATCC) (26) in 50 mM Tris, pH 8.3, 50 mM KCl, 10 mM MgCl_2 . Primer extension was initiated by the addition of 1 mM deoxynucleotides, 10 mM dithiothreitol, and 1 unit of avian myeloblastosis virus reverse transcriptase in a final volume of 26 μl followed by incubation of the mixture at 42 °C for 30 min. Products were separated on 8 M urea, 6% polyacrylamide gels and visualized by autoradiography. The precise location of the transcription initiation site was determined by comparing the migration of the major reverse transcription product with a dideoxy sequence ladder generated with the same oligonucleotide used for primer extension.

To identify the 3'-end of VEGF transcripts, a series of adjacent ^{32}P -labeled genomic DNA probes (probe A, 1.3-kb *EcoRI* fragment; probe B, 750-bp *EcoRI*-*SfiI* fragment; probe C, 600-bp *SfiI* fragment; see Fig. 7), spanning the 3'-end of the VEGF genomic clone, were hybridized to immobilized mouse lung RNA, according to standard protocols. Because of a weak, yet significant, hybridization signal, probe C was predicted to overlap regions of genomic DNA encoding the VEGF transcript and the 3'-flanking sequence. A nuclease protection assay was used to more precisely define the 3'-end. A 4.4-kb *SmaI* genomic DNA fragment (spanning the 3'-UTR and flanking region of VEGF) cloned in pBSII (Stratagene) was used for riboprobe synthesis. The DNA template was linearized at an *NcoI* site within the probe B region, and an antisense RNA probe of 2.2 kb (see Fig. 7) was transcribed with T7 RNA polymerase according to standard protocols (27). The probe was hybridized to C127I mouse mammary epithelial cell total RNA or yeast tRNA overnight at 30 °C in 40 mM PIPES, pH 6.4, 400 mM NaCl, 80% deionized formamide, 1 mM EDTA. The mixture was diluted in nuclease digestion buffer (50 mM sodium acetate, pH 5.0, 30 mM NaCl, 1 mM zinc acetate, 20 $\mu\text{g}/\text{ml}$ denatured calf thymus DNA) and then incubated in the presence of 300 units of mung bean nuclease (Life Technologies, Inc.) for 1 h at 30 °C. Reaction products were separated by denaturing gel electrophoresis in an 8 M urea, 4% polyacrylamide gel and visualized by autoradiography.

Mouse VEGF Promoter-Luciferase Constructs—A 1.6-kb fragment of VEGF genomic DNA, which encompasses 1.2 kb of the 5'-flanking sequence, the transcription start site, and 0.4-kb of corresponding 5'-UTR, was ligated upstream of a promoterless luciferase gene in the pGL2-basic plasmid (Promega). 5'-Deletions were made using convenient restriction sites within the VEGF promoter and the pGL2 multiple cloning site. These included a 445-bp deletion from the 5' terminus of the 1.6-kb fragment (−1217 bp) to the *ApaI* site at −772 bp, a 768-bp deletion from the 5' terminus to an internal *Mlu* site at −449 bp, and a 1.3-kb deletion from −1217 bp to the *SmaI* site at +126 bp (see Fig. 6). The promoterless plasmid, pGL2-basic, and a construct in which the promoter was cloned into pGL2-basic in opposite orientation with respect to transcription initiation served as negative controls. The human cytomegalovirus immediate early gene promoter/enhancer region was fused to the luciferase reporter for use as a positive control.

DNA Transient Transfection, Luciferase, and Alkaline Phosphatase Assays—Transient transfections were performed with 4 μg of test plasmid using Lipofectin (Life Technologies, Inc.) reagent according to the manufacturer's protocol. As a control for transfection efficiency, pRcCMVAP (4 μg), encoding a secreted placental alkaline phosphatase gene (kindly provided by Dr. Gerhard Raab, Children's Hospital, Boston), was cotransfected with test plasmids. Alkaline phosphatase activity was determined (28) and used to normalize luciferase assay values. Luciferase activity in cell extracts was assayed 48 h post-transfection according to standard protocols (27) using a Bioscan luminometer (Wallace).

neo/VEGF Fusion Constructs, Generation of Stable Cell Lines, and mRNA Stability Assays—A 4.4-kb *SmaI* fragment, encompassing 2 kb of the VEGF 3'-UTR, including poly(A) signals, and 2.4 kb of 3'-flanking sequence, was ligated into the *SmaI* site downstream of a neomycin resistance gene (*neo*) open reading frame in the eukaryotic expression plasmid LTR-*neo* (kindly provided by Dr. Michael Cole, Princeton University, Princeton, NJ). LTR-*neo* transcripts terminate with SV40 UTR and poly(A) sequences (29). LTR-*neo* and LTR-VEGF constructs were individually transfected by electroporation into C127I, a mammary epithelial cell line. The plasmid pPGKhyg, encoding the hygromycin resistance gene, was cotransfected with test plasmids to allow selection of stable transfectants with hygromycin (200 $\mu\text{g}/\text{ml}$). Stable colonies (50–100) were pooled and expanded for use in mRNA stability assays.

Actinomycin D chase assays and Northern blot analysis of total RNA were performed as described (20). Briefly, confluent cells were incubated in culture media containing actinomycin D (5 $\mu\text{g}/\text{ml}$) and subsequently incubated for 0–8 h in standard culture conditions. Total RNA was extracted by the modified acid-phenol method using RNazol B (Tel-test) and analyzed by Northern blot for LTR-*neo*, LTR-VEGF, and

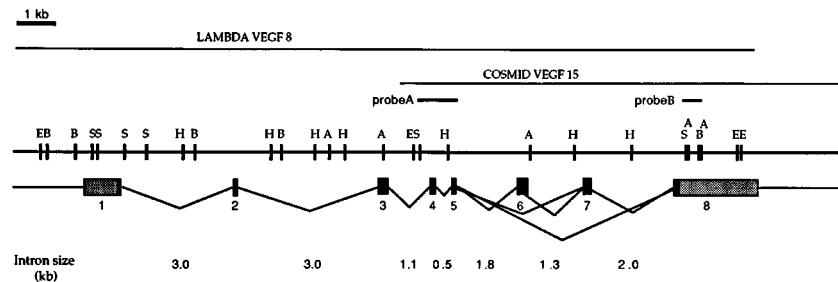


FIG. 1. **Genomic organization of mouse VEGF.** Restriction map of the mouse VEGF gene and flanking regions as established from the lambda 8 and cosmid 15 clones. Sites are marked for the enzymes *AccI* (A), *BamHI* (B), *EcoRI* (E), *HindIII* (H), and *SmaI* (S). Locations of exons 1–8 and intron sizes are indicated. The VEGF open reading frame is indicated by black shading.

β -actin mRNA levels. 15 μ g of RNA/sample were fractionated by denaturing gel electrophoresis and capillary blotted to charged nylon (GeneScreen Plus). Prehybridization and hybridization were carried out in $6 \times$ SSPE, $5 \times$ Denhardt's, 50% formamide, 1% SDS, and 100 μ g/ml sheared, denatured salmon sperm DNA. Probes for Northern blot analysis were random prime labeled with 32 P, using the following templates: a 280-bp fragment encoding exons 1–3 of the mouse VEGF cDNA open reading frame, a 440-bp *BssHII-SmaI* fragment of the *neo* gene, and a 400-bp fragment from the 3'-UTR of human β -actin (30).

RESULTS

Isolation and Preliminary Characterization of the Mouse VEGF Gene—To isolate the VEGF gene, a probe representing the mouse VEGF₁₆₄ open reading frame was used to screen a cosmid genomic DNA library prepared from strain 129 mouse liver. From an initial screen of 5×10^5 colonies, several positive clones were identified and analyzed further. Sequencing of the termini of cosmid inserts indicated that all of the clones originated within the middle of the VEGF coding region and proceeded approximately 30–40 kb in the 3' direction. Rescreening the cosmid library with the same probe, or a probe corresponding to the 5'-half of the VEGF open reading frame, did not identify cosmids harboring the 5'-end of the VEGF gene. Because the 5'-end of VEGF did not appear to be represented in the cosmid library, a 129 mouse genomic DNA library constructed using the EMBL3 lambda phage vector was screened. Using a probe spanning exons 1–3 to screen 1×10^6 plaques, two clones spanning the 5'-end of the VEGF gene were identified. One of these clones, designated lambda 8, also overlapped with regions represented in a VEGF cosmid clone (cos15); therefore, these two clones were used for structural analysis of the VEGF gene. The relation of the phage and cosmid clones to the mouse VEGF gene are shown schematically in Fig. 1.

A restriction map for the two overlapping clones was assembled by single, double, and partial digestions with *EcoRI*, *BamHI*, *AccI*, *HindIII*, and *SmaI* restriction enzymes (Fig. 1). The locations of exons relative to the restriction map were established by nucleotide sequencing the restriction sites proximal to exons and Southern blot analysis of cloned DNA with exon-specific probes (data not shown). Restriction enzyme analysis of genomic DNA by Southern blot was used to confirm mapping data and verified that mouse VEGF was encoded as a single copy gene (Fig. 2). The overlapping genomic clones define a contiguous stretch of 45 kb of DNA, of which approximately 14 kb represents the mouse VEGF coding region.

Exon-Intron Nucleotide Sequence and Organization—To determine the genomic organization of the mouse VEGF gene, nucleotide sequences of the coding regions and intron-exon borders were determined (Fig. 3) and aligned with published mouse VEGF cDNA sequences (4). Similar to the human gene, the coding region of mouse VEGF is interrupted by seven introns, with exons 1 and 8 containing relatively short segments of the coding region and the UTRs (22). The organization

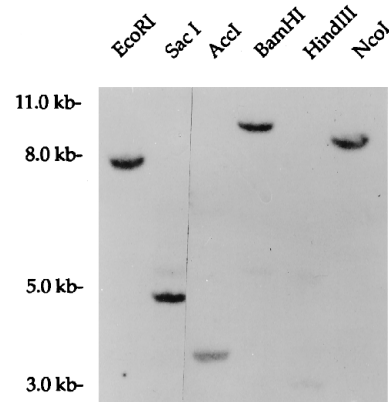


FIG. 2. **Genomic Southern blot analysis of mouse VEGF.** 129 mouse genomic DNA (10 μ g) was digested with the indicated enzymes and analyzed in a Southern blot using a mouse VEGF genomic DNA probe (probe A as illustrated in Fig. 1). The hybridizing fragment in *HindIII*-digested DNA is less than 3.0 kb in size and has been run from the gel.

of the mouse coding region suggests that the three VEGF protein isoforms, VEGF₁₂₀, VEGF₁₆₄, and VEGF₁₈₈, are created by alternative splicing of a single gene. The VEGF₁₈₈ splice variant includes all 8 exons, whereas the removal of exon 6 or both exons 6 and 7 yields the VEGF₁₆₄ and VEGF₁₂₀ splice variants, respectively. The mouse VEGF gene structure is shown schematically in Fig. 1.

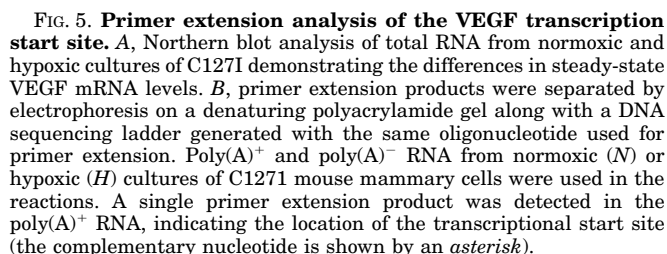
A fourth human VEGF isoform, designated VEGF₂₀₆, was previously identified by polymerase chain reaction amplification of VEGF isoforms from a fetal human liver cDNA library (31). From a comparison of cDNA and genomic sequence, this splice variant was predicted to be derived from the utilization of an alternative splice donor site downstream from the site originally identified for exon 6. The mouse gene would not be predicted to encode an isoform homologous to human VEGF₂₀₆. When compared to the published human sequence, the sequence of the corresponding region of the mouse gene contains an additional nucleotide, creating a frameshift that results in an in-frame stop codon (Fig. 4).

Functional Analysis of the Mouse VEGF Promoter—Alignment of sequences from the 5'-regions of mouse and human VEGF and primer extension analysis were used to map the site of transcriptional initiation for VEGF mRNA in the C127I mouse mammary epithelial cell line. Low levels of VEGF mRNA were detectable in the C127I cells grown under typical culture conditions, but were dramatically induced by exposing the cells to a low oxygen environment (Fig. 5A). An antisense primer, predicted to anneal approximately 100 nucleotides downstream of the transcription initiation region, was chosen based on alignment of the human proximal promoter region with corresponding mouse sequence. The primer was annealed to poly(A)⁺ RNA isolated from normoxic and hypoxic cultures

FIG. 3. Nucleotide sequence for mouse VEGF intron-exon borders and the sequence surrounding the mouse VEGF transcription initiation site. Intron and UTR sequence is shown in lower case letters, coding sequence is shown in upper case letters, and the VEGF translation start and stop codons are boxed. An arrow indicates the initiation site of RNA synthesis and is designated +1. Consensus binding sites for relevant transcription factors are marked as follows: AP-1, thin line; AP-2, heavy hatched line; NFkB, broken line; Sp1, heavy line.

TAC GTT GGT GCC CGC TGC TGT CTA ATG CCC TGG AGC CTC CCT GGC...
Y V G A R C C L M P W S L P G....

of C127I. Primer extension using poly(A)⁻ RNA was used as a negative control. After reverse transcription and denaturing gel electrophoresis, a single abundant primer extension product of 123 bp was detected in the mRNA from hypoxic cell cultures (Fig. 5B). As would be expected, significantly lower levels of reaction product were seen in mRNA from normoxic cultures or in poly(A)⁻ RNA from normoxic and hypoxic cultures. The precise location of transcription initiation was determined by comparison of the migration of the extension prod-



The murine astrocytoma cell line, C6, was transiently transfected with reporter constructs, and cell extracts were assayed for luciferase activity 48 h post-transfection. VEGF sequences fused to the reporter in the appropriate transcriptional orientation consistently produced a 7-fold increase in luciferase activity when compared to a promoterless luciferase construct (Fig. 6). In contrast, VEGF sequences fused in the opposite transcriptional orientation did not induce a significant level of reporter activity. Deletion of 445 or 770 bp from the 5'-end of

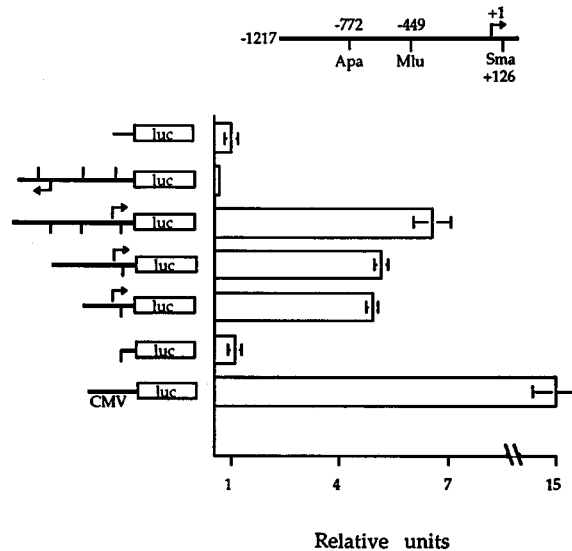


FIG. 6. **Functional analysis of the mouse VEGF promoter.** Relative luciferase activities were obtained from transiently transfected VEGF promoter-luciferase constructs in C6 glioma cells. Schematic representation of assay constructs (see "Materials and Methods") is shown. All luciferase values were normalized for transfection efficiency, using placental alkaline phosphatase activity, and are expressed as the level of luciferase activity relative to the activity of the promoterless luciferase control plasmid pGL2 basic. Data shown are from duplicate analyses and are representative of five separate experiments. Within these five experiments, peak VEGF promoter activity varied from 7 to 10-fold relative to negative controls.

the promoter fragment resulted in a 25% decrease in reporter activity, whereas a 1.3-kb deletion, which removed putative promoter sequences and the transcriptional initiation site, reduced luciferase activity to background levels.

Identification of the VEGF Transcription Termination Region—The region of transcriptional termination for VEGF was mapped by RNA hybridization and nuclease protection assays. First, to approximate the junction of the VEGF 3'-UTR and the 3'-flanking region, genomic probes spanning the putative 3'-region of the VEGF gene were used in a slot blot hybridization analysis of mouse VEGF RNA (Fig. 7A). Independent hybridization of all three probes to the mouse RNA resulted in detectable, though variable, signal (Fig. 7B). No signal was detected in hybridizations to a yeast tRNA negative control. Relative to probes A and B, probe C weakly hybridized to immobilized mouse RNA. From the dramatic decrease in hybridization signal seen for probe C, it was predicted that this region of DNA spanned the junction of VEGF transcriptional termination and the non-transcribed 3'-flanking region.

Nuclease protection analysis of mRNA from C127I cells was used to obtain more precise information on the 3'-end of VEGF transcripts. A 2.2-kb radiolabeled antisense riboprobe was generated from a genomic DNA template and hybridized to total RNA from hypoxic and normoxic cultures of C127I and a yeast tRNA negative control. Following nuclease digestion and electrophoretic separation of nuclease products, a 510–520-nucleotide nuclease-resistant species was observed in hypoxic RNA hybrids (Fig. 7C). The same protected fragment was observed from normoxic RNA hybrids after extended exposures of the analytical gel, reflecting the 10–20-fold differences in VEGF mRNA levels between normoxic and hypoxic cultures. The faint band of about 450 bp may reflect the existence of a less utilized alternative termination site. No product was seen in the yeast tRNA negative control. These data place the site of transcriptional termination approximately 510 bp downstream from the riboprobe terminus, leading to a 3'-UTR of approximately 2.2 kb.

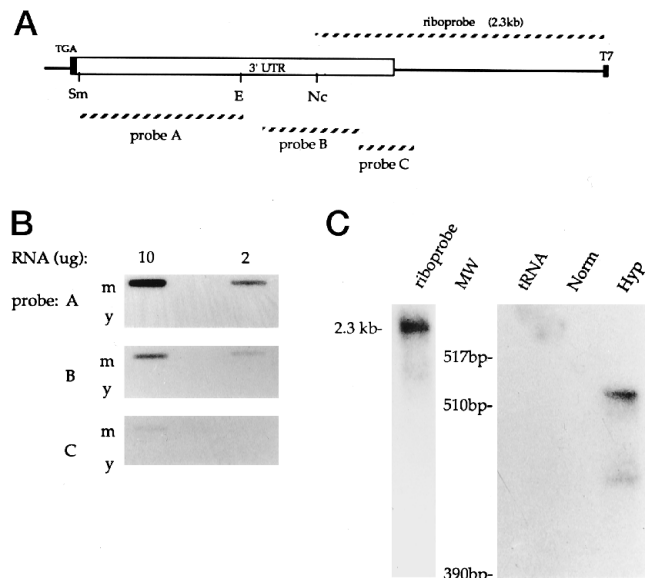


FIG. 7. **Analysis of the mouse VEGF 3'-end.** A, schematic of exon 8 and corresponding flanking region. *EcoRI* (E), *SmaI* (S), and *NcoI* (Nc) restriction sites are marked. Regions corresponding to 3'-UTR probes A, B, and C and the T7-synthesized riboprobe are indicated. B, slot-blot hybridization analysis of 10 or 2 μ g of mouse total RNA (m) and control yeast tRNA (y) with 3'-UTR probes. C, analysis of mung bean nuclease-digested C127I RNA/riboprobe hybrids. A 510–520-nucleotide digestion-resistant product is present solely in total RNA from hypoxic C127I cultures.

Identification of VEGF mRNA Destabilizing Sequences—We have previously demonstrated that VEGF mRNA from cells grown under normoxic conditions is highly unstable, with a half-life of <1 h (20). Whereas the average half-life of cellular mRNAs is approximately 8 h, the mRNAs for many growth factors and oncoproteins (e.g. granulocyte-macrophage colony stimulating factor, *c-fos*, *c-myc*) are unstable, with half-lives ranging from 20 to 60 min. The signals responsible for destabilization of these mRNAs are most frequently located in the 3'-UTR (29, 32).

To investigate if a determinant of mRNA destabilization is present in the VEGF 3'-UTR, genomic sequences corresponding to this region, including the putative polyadenylation signal, were fused to a neomycin (*neo*) reporter mRNA (designated LTR-VEGF). The VEGF 3'-UTR replaces SV40 DNA sequences that normally terminate the *neo* transcripts. The *neo*/SV40 mRNA fusion (designated LTR-*neo*) is normally quite stable, with a half-life of >8 h. The addition of destabilization sequences from the 3' UTR of granulocyte-macrophage colony stimulating factor, *c-fos*, and *c-myc* to LTR-*neo* mRNA has been shown to direct its rapid decay (29).

Actinomycin D chase studies were used to compare the rate of decay for LTR-VEGF mRNA to that of LTR-*neo* mRNA (control) in the C127I mammary epithelial cell line. As expected, the control LTR-*neo* mRNA remained stable throughout an 8-h period in the absence of transcription (Fig. 8). In contrast, LTR-VEGF fusion mRNA behaved similar to the endogenous VEGF mRNA, with both VEGF and LTR-VEGF transfectants undergoing rapid decay with half-lives of less than 1 h. Levels of endogenous β -actin mRNA, a transcript with an average half-life, were relatively stable under each experimental condition over the time course of the experiment (33).

DISCUSSION

VEGF has been implicated as a multi-functional effector of vascular cell function. In addition to its well documented angiogenic properties, VEGF is also a potent stimulator of leuko-

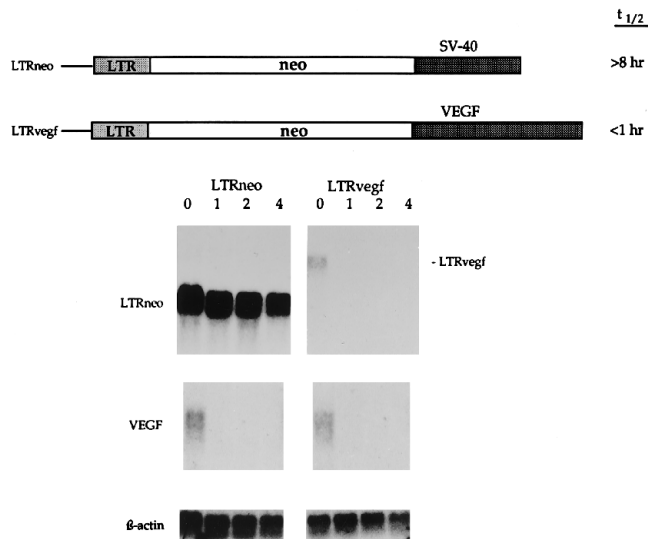


FIG. 8. The VEGF 3'-UTR contains a region that promotes destabilization of a normally stable fusion mRNA. LTR-*neo* and LTR-VEGF transfectants (schematic of fusion mRNA constructs shown; see "Materials and Methods") were used to analyze *neo* fusion mRNA, VEGF mRNA, and β -actin mRNA decay using an actinomycin D chase protocol. Time (h) after the addition of actinomycin D is marked above each lane.

cyte migration, vascular permeability, and procoagulant functions in endothelium (34, 35). Moreover, the presence of significant VEGF mRNA and protein in various tissues of the adult suggests an additional role for VEGF in the maintenance of normal vascular cell integrity and/or behavior (4). How VEGF gene expression is regulated during the transition from periods of vascular quiescence to active vascular growth, remodeling, and repair is not understood. To begin to investigate the structure-function relationships critical for the regulation of VEGF expression, we have characterized the mouse VEGF gene.

Mapping the VEGF Transcriptional Unit—We have isolated genomic clones encompassing the VEGF gene, as well as 1.2 kb of 5'-flanking sequence and more than 25 kb of 3'-flanking sequence. Similar to the human gene, the mouse VEGF coding region is distributed across 8 exons, spanning 14 kb of genomic sequence. Exons 1 and 8 contain the translation start and stop codons, respectively, and the extensive UTR regions. Sequence data and primer extension analysis of the transcription initiation site indicate that the mouse VEGF gene, like the human, has an unusually large 5'-UTR of approximately 1.0 kb (22). The site of VEGF transcription termination had not been previously defined for any of the VEGF genes; therefore, the size of the mouse 3'-UTR and approximate site of poly(A) addition were determined. Results from nuclease protection analysis revealed that the site of VEGF transcriptional termination is approximately 2.2 kb downstream from the end of the VEGF open reading frame. Including a 1.0-kb 5'-UTR, a coding region of 0.5–0.6 kb, and a 3'-UTR of 2.2 kb, the size of a VEGF transcript predicted by mapping data would be 3.7–3.9 kb, a size corresponding to the sizes of the most commonly observed VEGF transcripts (36).

Genomic Organization of VEGF Splice Variants—Details of the exon-intron structure for mouse VEGF suggest that alternative splicing generates the mRNAs that encode the 120-, 164-, and 188-amino acid isoforms of VEGF similar to the human gene (22). Yet, unlike human VEGF, the sequence structure of mouse exon 6 does not support the existence of a mouse equivalent to the human VEGF₂₀₆ isoform. An in-frame stop codon is present in the mouse gene in the region corre-

sponding to the human VEGF₂₀₆ open reading frame. If synthesized and translated, mouse VEGF splicing variants that include this region would be predicted to produce a novel, secreted VEGF protein isoform of approximately 16 kDa. The existence of this mRNA or protein has not been described.

Since little is known about the physiological roles of the four VEGF isoforms, it is difficult to predict the functional significance of a divergence in isoform generation between humans and mice. The putative VEGF₂₀₆ isoform was identified using the polymerase chain reaction to amplify VEGF-related cDNAs and consists of an alternative splice variant with an extended exon 6 region that results in a 17-amino acid insertion relative to the VEGF₁₈₉ isoform. Analysis of VEGF synthesis, secretion, and bioactivity *in vitro* has revealed that an engineered VEGF₂₀₆ protein shares similar biochemical and functional properties with VEGF₁₈₉, suggesting that these two isoforms could provide redundant biological functions (31). To date, the biochemical and biological descriptions of VEGF₂₀₆ have been sparse and have relied on data obtained from the fusion of the N-terminal region of VEGF₁₆₅ to the partial VEGF₂₀₆ cDNA clone; the expression of native VEGF₂₀₆ mRNA or protein by tissue culture cells or *in vivo* has not been adequately described.

VEGF Promoter Analysis—Similar to other growth-related genes, including human VEGF, consensus TATA and CCAAT sequences for RNA polymerase II-initiated transcription are absent from the mouse VEGF core promoter region. Instead, GC-rich regions resembling consensus binding motifs for Sp1 are situated approximately 50–80 bp upstream of the predicted transcription start site in mouse VEGF. This organization is typical of the core region of many TATA-less promoters, which usually contain binding sites for sequence-specific transcriptional activators, frequently Sp1, and an initiator element (Inr) that overlaps the region of RNA synthesis (37, 38). The nucleotide sequence surrounding the VEGF mRNA initiation site, AGAAGCGCA (underline designates first transcribed nucleotide), does not conform to consensus Inr sequences; therefore, an investigation of VEGF transcriptional initiation is likely to shed light on a novel "TATA-less" mechanism for basal gene transcription (39).

Transient transfection assays indicate that a 1.2-kb segment of 5'-flanking region specifically directs the transcription of a reporter gene in VEGF-producing cells. Deletion of the 1.2-kb region, including the putative transcription initiation site, abolished promoter activity. Results from these functional analyses support transcript mapping and sequence analysis data that identify this DNA segment as the VEGF proximal promoter.

Transfection of C6 rat glioma with constructs deleting either 445 or 770 bp from the 5'-end of the 1.2-kb promoter region resulted in a similar 25% decrease in reporter activity, suggesting that cis-acting elements necessary for basal promoter activity in C6 cells reside in the 450-bp DNA segment deleted from the 5'-end of the promoter fragment. Yet, a relevant promoter activity resides within the first 450 bp upstream to the VEGF gene. Further studies will be required to identify and characterize the cis- and trans-acting components necessary for both basal and inducible regulation of VEGF gene transcription.

Sequence analysis of the 1.2-kb region, upstream of the transcription initiation site, revealed the presence of a number of potential cis-acting regulatory elements. Similar to the human VEGF gene, multiple consensus binding sites for AP-1 and AP-2 transactivating complexes are present. AP-1 activity has been shown to be stimulated by phorbol esters and growth factors, and both cAMP-dependent kinase and protein kinase C

pathways have been implicated in the activation of AP-2 (40, 41). Phorbol esters, peptide growth factors, and intracellular elevation of cAMP also induce steady-state VEGF mRNA, suggesting that the AP-1 and AP-2 consensus sites present in the VEGF promoter may mediate VEGF transcriptional activation in response to these effectors (17, 21). In addition, studies from a number of laboratories indicate that in some cells transcriptional activation plays a role in the up-regulation of VEGF mRNA by hypoxia (42–44). Further, the site of transcriptional initiation and numerous regions within the proximal promoter of mouse VEGF share significant similarity in both sequence and organization with the human homologue. The conserved organization of transcriptional regulatory sequences within the two promoters may imply a critical role for these regions in the proper regulation of VEGF gene expression. In contrast, consensus sites for NFkB, a transactivator implicated in the regulation of inflammation and stress response genes (45), are located 90 and 185 bp upstream of the initiation site in mouse VEGF, whereas NFkB consensus sites have not been identified in the human VEGF promoter.

Control of VEGF mRNA Stability—In addition to transcriptional control of gene expression, the level of mRNA for many oncoproteins and cytokines is regulated by post-transcriptional control of mRNA stability. For the best-studied of these genes, including granulocyte-macrophage colony stimulating factor and *c-myc*, the 3'-UTR is primarily responsible for the control of mRNA stability (29, 32). Results from our analysis of VEGF mRNA stability indicate that the VEGF 3'-UTR functions in an analogous fashion. Fusion of genomic DNA, representing the VEGF 3'-UTR, to a normally stable *neo* reporter gene destabilizes the transcripts, reducing the half-life from >8 h to less than 1 h. In contrast, LTR-*neo* and endogenous β -actin mRNAs were stable throughout the experimental time course, confirming that specific cellular mRNAs are targeted for destruction.

Experimental conditions that induce VEGF mRNA, such as phorbol ester treatment or hypoxia, are known to regulate mRNA stability (20, 32). Investigation of the cellular mechanisms controlling transcript stability suggest that certain mRNAs contain distinct structural elements for positive and negative regulation of mRNA stability. Specific destabilization sequences vary considerably but usually consist of AU-rich elements in the 3'-UTR of unstable mRNAs (46). Multiple AU-rich regions exist throughout the 3'-UTR of mouse VEGF (data not shown) and represent potential candidates for destabilizing sequences. Less is known about sequences that selectively or inducibly promote mRNA stability. For the transferrin receptor, a well studied model of inducible mRNA stability, the 3'-UTR contains a stem-loop sequence that interacts with inducible cellular factors to promote mRNA stability (47). During periods of iron starvation, RNA-protein interactions at the stem-loop sequence are dominant over the effects of a distinct region of AU-containing sequences, which otherwise trigger transferrin receptor mRNA degradation (48). Further investigation will be required to define sequences within the VEGF mRNA required for positive and negative regulation of post-transcriptional mRNA stability.

The findings reported here provide a framework for the comprehensive analysis of the regulation of VEGF expression and VEGF structure-function relationships. Such studies will be critical to understanding and eventually modulating the role of VEGF during physiological and pathological blood vessel growth.

REFERENCES

- Folkman, J. (1995) *Nature Med.* **1**, 27–31
- Leung, D. W., Cachianes, G., Kuang, W. J., Goeddel, D. V., and Ferrara, N. (1989) *Science* **246**, 1306–1309
- Senger, D. R., Galli, S. J., Dvorak, A. M., Perruzzi, C. A., Harvey, V. S., and Dvorak, H. F. (1983) *Science* **219**, 983–985
- Breier, G., Albrecht, U., Sterrer, S., and Risau, W. (1992) *Development* **114**, 521–532
- Shweiki, D., Itin, A., Neufeld, G., Gitay-Goren, H., and Keshet, E. (1993) *J. Clin. Invest.* **91**, 2235–2243
- Miller, J. W., Adamis, A. P., Shima, D. T., D'Amore, P. A., Moulton, R. S., O'Reilly, M. S., Folkman, J., Dvorak, H. F., Brown, L. F., Berse, B., Yeo, T.-K., and Yeo, K.-T. (1994) *Am. J. Pathol.* **145**, 574–584
- Kim, K. J., Li, B., Winer, J., Armanini, M., Gillett, N., Phillips, H. S., and Ferrara, N. (1993) *Nature* **362**, 841–844
- Millauer, B., Shawver, L. K., Risau, W., and Ullrich, A. (1994) *Nature* **367**, 576–579
- Adamis, A. P., Shima, D. T., Tolentino, M., Gragoudas, E., Ferrara, N., Folkman, J., D'Amore, P. A., and Miller, J. W. (1995) *Arch. Ophthalmol.*, in press
- Pierce, E. A., Avery, R. L., Foley, E. D., Aiello, L. P., and Smith, L. E. H. (1995) *Proc. Natl. Acad. Sci. U. S. A.* **92**, 905–909
- Millauer, B., Witzmann-Voss, S., Schnürch, H., Martinez, R., Möler, N. P. H., Risau, W., and Ullrich, A. (1993) *Cell* **72**, 835–846
- Peters, K. G., De Vries, C., and Williams, L. T. (1993) *Proc. Natl. Acad. Sci. U. S. A.* **90**, 8915–8919
- Dumont, D. J., Fong, G.-H., Puri, M. C., Gradwohl, G., Alitalo, K., and Breitman, M. L. (1995) *Dev. Dynamics* **203**, 80–92
- Shalaby, F., Rossant, J., Yamaguchi, T. P., Gertsenstein, M., Wu, X.-F., Breitman, M., and Schuh, A. C. (1995) *Nature* **376**, 62–64
- Fong, G.-H., Rossant, J., Gertsenstein, M., and Breitman, M. L. (1995) *Nature* **376**, 66–68
- Klagsbrun, M., and Soker, S. (1994) *Curr. Biol.* **3**, 699–702
- Garrido, G., Saule, S., and Gospodarowicz, D. (1993) *Growth Factors* **8**, 109–117
- Shweiki, D., Neeman, M., Itin, A., and Keshet, E. (1995) *Proc. Natl. Acad. Sci. U. S. A.* **92**, 768–772
- Goldberg, M. A., and Schneider, T. J. (1994) *J. Biol. Chem.* **269**, 4355–4359
- Shima, D. T., Deutsch, U., and D'Amore, P. A. (1995) *FEBS Lett.* **370**, 203–208
- Finkenzeller, G., Technau, A., and Marme, D. (1995) *Biochem. Biophys. Res. Commun.* **208**, 432–439
- Tischer, E., Mitchell, R., Hartman, T., Silva, M., Gospodarowicz, D., Fiddes, J. C., and Abraham, J. A. (1991) *J. Biol. Chem.* **266**, 11947–11954
- Herrmann, B. G., and Frischauf, A. (1987) in *Guide to Molecular Cloning Techniques* (Berger, S. L., and Kimmel, A. L., eds) **Vol. 152**, pp. 180–183, Academic Press, San Diego
- Chomczynski, P., and Sacchi, N. (1987) *Anal. Biochem.* **162**, 156–159
- Sambrook, J., Fritsch, E. F., and Maniatis, T. (1989). *Molecular Cloning: A Laboratory Manual*, Cold Spring Harbor Laboratory Press, Cold Spring Harbor, NY
- Shima, D. T., Adamis, A. P., Yeo, K.-T., Yeo, T.-K., Allende, R., Folkman, J., and D'Amore, P. A. (1995) *Mol. Med.* **1**, 182–193
- Ausubel, F. M., Brent, R., Kingston, R., Moore, D., Seidman, J., Smith, J., and Struhl, K. (eds) (1987) *Current Protocols in Molecular Biology*, John Wiley & Sons, Inc., New York
- Berger, J., Hauber, J., Hauber, R., Geiger, R., and Cullen, B. (1988) *Gene (Amst.)* **66**, 1–10
- Schuler, G. D., and Cole, M. D. (1988) *Cell* **55**, 1115–1122
- Hoock, T. C., Newcomb, P. M., and Herman, I. M. (1991) *J. Cell Biol.* **112**, 653–664
- Houck, K. A., Ferrara, N., Winer, J., and Cachianes, G. (1991) *Mol. Endocrinol.* **5**, 1806–1814
- Shaw, G., and Kamen, R. (1986) *Cell* **46**, 659–667
- Hargrove, J. L., and Schmidt, F. H. (1989) *FASEB J.* **3**, 2360–2370
- Ferrara, N., Houck, K., Jakeman, L., and Leung, D. W. (1992) *Endocr. Rev.* **13**, 18–32
- Senger, D. R., Van De Water, L., Brown, L. F., Nagy, J. A., Yeo, K.-T., Yeo, T.-K., Berse, B., Jackman, R. W., Dvorak, A. M., and Dvorak, H. F. (1993) *Cancer Met. Rev.* **12**, 303–324
- Adamis, A. P., Shima, D. T., Yeo, K.-T., Yeo, T.-K., Brown, L. F., Berse, B., D'Amore, P. A., and Folkman, J. (1993) *Biochem. Biophys. Res. Commun.* **193**, 631–638
- Azizkhan, J., Jensen, D., Pierce, A., and Wade, M. (1993) *Crit. Rev. Eukaryotic Gene Expression* **3**, 229–254
- Boisclair, Y., Brown, A., Casola, S., and Rechler, M. (1993) *J. Biol. Chem.* **268**, 24892–24901
- Zawel, L., and Reinberg, D. (1992) *Curr. Opin. Cell Biol.* **4**, 488–495
- Curran, T., and Franz, B. R. (1988) *Cell* **55**, 395–397
- Imagawa, M., Chiu, R., and Karin, M. (1987) *Cell* **51**, 251–260
- Minchenko, A., Salceda, S., Bauer, T., and Caro, J. (1994) *Cell. Mol. Biol. Res.* **40**, 35–39
- Ikeda, E., Achen, M. G., Breier, G., and Risau, W. (1995) *J. Biol. Chem.* **270**, 19761–19766
- Liu, Y., Cox, S. R., Morita, T., and Kourembanas, S. (1995) *Circ. Res.* **77**, 638–643
- Read, M. A., Whitley, M. Z., Williams, A. J., and Collins, T. (1994) *J. Exp. Med.* **179**, 503–512
- Chen, C., and Shyu, A. (1994) *Mol. Cell. Biol.* **14**, 8471–8482
- Koeller, D. M., Casey, D. M., Hentze, E. M., Chan, L.-N., Klausner, R. D., and Harford, J. B. (1989) *Proc. Natl. Acad. Sci. U. S. A.* **86**, 3574–3578
- Casey, J. L., Di Jeso, B., Rao, K., Klausner, R. D., and Harford, J. B. (1988) *Proc. Natl. Acad. Sci. U. S. A.* **85**, 1787–1791